Fungal Genetics and Biology 91 (2016) 32–42

Contents lists available at ScienceDirect

Fungal Genetics and Biology

journal homepage: www.elsevier.com/locate/yfgbi

A cytoplasmic Cu-Zn superoxide dismutase SOD1 contributes to hyphal growth and virulence of *Fusarium graminearum*

Sheng-Hua Yao [a,b,1], Yan Guo [a], Yan-Zhang Wang [a], Dong Zhang [a], Ling Xu [b], Wei-Hua Tang [a,*]

[a] National Key Laboratory of Plant Molecular Genetics, Center for Excellence in Molecular Plant Sciences, Institute of Plant Physiology and Ecology, Shanghai Institutes for Biological Sciences, Chinese Academy of Sciences, Shanghai 200032, China
[b] School of Life Science, East China Normal University, Shanghai 200062, China

ARTICLE INFO

Article history:
Received 6 October 2015
Revised 18 February 2016
Accepted 25 March 2016
Available online 29 March 2016

Keywords:
Cu-Zn SOD1
Reactive oxygen species (ROS)
Fusarium graminearum
Pathogenicity
Hyphal growth
Deoxynivalenol

ABSTRACT

Superoxide dismutases (SODs) are scavengers of superoxide radicals, one of the main reactive oxygen species (ROS) in the cell. SOD-based ROS scavenging system constitutes the frontline defense against intra- and extracellular ROS, but the roles of SODs in the important cereal pathogen *Fusarium graminearum* are not very clear. There are five *SOD* genes in *F. graminearum* genome, encoding cytoplasmic Cu-Zn SOD1 and MnSOD3, mitochondrial MnSOD2 and FeSOD4, and extracellular CuSOD5. Previous studies reported that the expression of *SOD1* increased during infection of wheat coleoptiles and florets. In this work we showed that the recombinant SOD1 protein had the superoxide dismutase activity *in vitro*, and that the SOD1-mRFP fusion protein localized in the cytoplasm of *F. graminearum*. The Δ*sod1* mutants had slightly reduced hyphal growth and markedly increased sensitivity to the intracellular ROS generator menadione. The conidial germination under extracellular oxidative stress was significantly delayed in the mutants. Wheat floret infection assay showed that the Δ*sod1* mutants had a reduced pathogenicity. Furthermore, the Δ*sod1* mutants had a significant reduction in production of deoxynivalenol mycotoxin. Our results indicate that the cytoplasmic Cu-Zn SOD1 affects fungal growth probably depending on detoxification of intracellular superoxide radicals, and that SOD1-mediated deoxynivalenol production contributes to the virulence of *F. graminearum* in wheat head infection.

1. Introduction

Fusarium graminearum is an ascomycetous fungus that can cause Fusarium head blight (FHB) on wheat and barley, stalk and ear rot diseases on maize, as well as seedling blight on maize and wheat (Goswami and Kistler, 2004; Kazan et al., 2012; Dal Bello et al., 2002). This fungus not only causes crop yield loss, but also contaminates grain with its mycotoxins such as deoxynivalenol (DON) that are harmful to humans and animals. In the course of infection, this pathogen to varying degrees is confronted with host-derived reactive oxygen species (ROS) as well as ROS produced by fungal cell metabolic process (Ponts et al., 2007; Zhang et al., 2012). The regulation of cellular levels of ROS is critical for developmental differentiation and virulence of many pathogenic fungi (Gessler et al., 2007; Kim et al., 2009). Excess ROS such as superoxide anions ($O_2^{\cdot-}$), hydroxyl radicals ($OH^{\cdot}$) and hydrogen peroxide (H_2O_2) can react nonspecifically and rapidly with macromolecules, including DNA, proteins, lipids, and carbohydrates. These reactions can cause molecular damage such as DNA mutations, lipid peroxidation, and protein oxidations, leading to cellular dysfunction and eventually organismal death (Halliwell and Gutteridge, 2015). To cope with the effect of ROS in cells, all living organisms have developed a complex ROS scavenging system to detoxify elevated intracellular ROS levels. Generally, ROS scavenging systems can be divided into enzymatic and nonenzymatic systems. Nonenzymatic defense systems typically comprise small soluble molecules that are oxidized by ROS and thereby remove oxidants from solution. They include the major cellular redox buffer glutathione (GSH, a tripeptide γ-L-glutamyl-L-cysteinyl-glycine), and other compounds like phytochelatins, ascorbic acid, polyamines, flavonoids, alkaloids, and carotenoids. Enzymatic ROS scavenging mechanisms include superoxide dismutase (SOD) and various peroxidases, such as catalase (CAT), glutathione peroxidase (GPX) and ascorbate peroxidase (APX) (Apel and Hirt, 2004). The SODs act as the first line of defense against ROS, as their function is to dismutate superoxide anion radical into

* Corresponding author at: 300 Fenglin Road, Shanghai 200032, China.
E-mail address: whtang@sibs.ac.cn (W.-H. Tang).
[1] Present address: Shanghai High School International Division, Shanghai 200231, China.

http://dx.doi.org/10.1016/j.fgb.2016.03.006
1087-1845/

hydrogen peroxide and molecular oxygen (Fridovich, 1995). Then CAT, GPX and APX detoxify hydrogen peroxide subsequently. Several lines of evidence have confirmed that ROS scavenging systems are crucial for suppressing toxic ROS levels in a cell and are also regulated tightly (Hasan et al., 2002; Yamamoto et al., 2007; Kim et al., 2009). In *F. graminearum*, what constitutes the ROS scavenging system and how ROS are removed including intracellular ROS produced by itself as well as host-generated ROS during interaction are still not well understood.

SODs work as scavengers of superoxide, ubiquitously present in both prokaryotes and eukaryotes where they function to protect the cells from endogenously generated superoxide anions during aerobiosis (Fridovich, 1995). SODs are metalloenzymes that are broadly classified based on the metal cofactor used. On the basis of their binding of metal co-factor, SODs are classified into four types: manganese co-factored (MnSOD), iron co-factored (FeSOD), copper-zinc co-factored (Cu-ZnSOD) and nickel co-factored (NiSOD) (Fridovich, 1995; Youn et al., 1996). These different types of SODs are localized in different cellular compartments. MnSOD is mainly present in mitochondria and peroxisomes. FeSOD has been detected mainly in chloroplasts but also has been detected in peroxisomes, and Cu-ZnSOD has been detected in cytosol, chloroplasts, peroxisomes, and apoplast (Valentine et al., 2005). The compartmentalization of different forms of SOD throughout organisms allows them counteract various stresses locally. SOD outcompetes damaging reactions of superoxide, thus protecting the cell from superoxide toxicity. Besides serving as a key antioxidant for detoxification of the radicals that are normally produced within cells, SOD has been showed to be important for bacterial and fungal development and pathogenesis (Lynch and Kuramitsu, 2000; Poyart et al., 2001; Hwang et al., 2003; Aguirre et al., 2005; Narasipura et al., 2005; Abba et al., 2009; Lambou et al., 2010; Tang et al., 2012; Heindorf et al., 2014; Li et al., 2015).

During the interactions of *F. graminearum* and hosts, ROS are accumulated at the infected site, suggesting ROS are involved in this fungus-plant interaction (Zhang et al., 2012). The release of genome sequence of *F. graminearum* and a recent study revealed that there are many genes related to intracellular and extracellular ROS production and scavenging (Ma et al., 2010; Zhang et al., 2012). The analyses of expression profiles during wheat coleoptile infection indicate that *F. graminearum* primarily scavenges extracellular ROS before later production of extracellular ROS (Zhang et al., 2012). To elucidate the specific roles of SODs in *F. graminearum* and gain insights into the specific mechanisms of ROS participating in *F. graminearum* infection of wheat, we identified all *SOD*s in *F. graminearum* and focused on characterization of a Cu-ZnSOD, named SOD1, which expressed at high levels *in vitro* growth and during infection process. Data presented here show that SOD1 is the scavenger of the intracellular superoxide anions. Although dispensable for hyphal morphology and conidiation, SOD1 is important for conidial germination under extracellular ROS, for the DON production, and for the virulence on infection of wheat florets.

2. Materials and methods

2.1. Strains and culture conditions

The *F. graminearum* wild-type strain PH-1 (NRRL 31084), all mutants, complemented transformants, AmCyanPH-1 harboring the constitutively expressed AmCyan protein (Yuan et al., 2008; Zhang et al., 2012), and AmCyan*Δsod1* harboring constitutively expressing AmCyan in this study were routinely cultured at 25 °C on V8 agar. The wild-type strain and its derived mutants were incubated in mung bean broth (MBB) for conidial preparation, and conidial suspension for inoculation were prepared as described previously (Zhang et al., 2012).

2.2. Enzyme activity assay

The full-length cDNA of *SOD1* were cloned into pET-28a(+), and the resulting construct was transformed into *Escherichia coli* BL21. The transformed strain was incubated in Luria–Bertani broth (plus 50 mg/L kanamycin) to log phase ($OD_{600} \approx 0.8$) at 37 °C with shaking at 200 rpm. The expression of recombinant proteins was induced by adding 0.5 mM isopropyl-B-D-thio-galactopyranoside (IPTG) and followed by 8 hours' culture at 18 °C. SDS-PAGE analyses were used to examine the crude protein extracts and purified proteins. The enzyme activity of SOD1 was verified by measuring its inhibitory effect on the process of xanthine oxidase catalyzing xanthine to generate superoxide anion free radicals, and then the superoxide radicals could oxidize hydroxylamine to generate nitrite which reacts with developer to give a purple color. Based on this principle, we used a Cu-Zn SOD activity assay kit A001-2 (Nanjing Jiancheng Bioengineering Research Institute) to determine the SOD1 activity. The detailed procedures were performed as the manufacture's instruction. One unit of SOD activity was defined as the SOD amount required to inhibit 50% xanthine oxidation rate and expressed as U/mg proteins.

2.3. The expression analyses of SOD genes

The microarray data on the conidial germination at different stages (Experiment FG7), during wheat coleoptile infection (Experiment FG19), wheat head blight (Experiment FG15) and crown rot disease of wheat (Experiment FG12) were downloaded from Plexdb (Seong et al., 2008; Stephens et al., 2008; Lysoe et al., 2011; Zhang et al., 2012). Expression heatmaps were generated in R using the 'heatmap' function of the BioConductor amap package.

2.4. RNA extraction, amplification and quantitative PCR

Total RNA samples of *F. graminearum* infection of wheat coleoptiles at 16, 40 and 64 h after inoculation (hai) were extracted from laser microdissected tissues and amplified to complementary RNA (cRNA) as previous reported (Zhang et al., 2012). For *in vitro*-cultured conidia and hyphae grown for 72 h, total RNA was extracted using EasyPure Plant RNA Kit (Transgen Biotech), diluted to 1 ng/μL and amplified to cRNA as above. For quantitative PCR assays, approximately 1000 ng cRNA was used to synthesize cDNA with EasyScriptFisrt-Strand cDNA Synthesis SuperMix Kit (Transgen Biotech) using random primers. Real-time PCR was performed using Bio-Rad IQ double-color real time PCR detection system with the Transcript Green One-Step qRT-PCR SuperMix Kit (Transgen Biotech). The program used includes initial denaturation step at 95 °C for 30 s and 40 amplification cycles at 95 °C for 5 s and 60 °C for 30 s. Data was analyzed with the Bio-Rad CFX Manage Software (Bio-Rad) with the tubulin gene FGSG_09530 as a reference. The primers are listed in Table S1.

2.5. The analysis of SOD1 subcellular localization

To generate constitutively expressed SOD1-mRFP, full-length cDNA of *SOD1* was cloned into the *vma3* promoter-mRFP vector (Yuan et al., 2008). The construct were then transformed into the protoplasts of the wild-type strain. Transformants expressing the SOD1-mRFP construct were confirmed by PCR. Transgenic *F. graminearum* AmCyanPH-1 was used for the control (Yuan et al., 2008; Zhang et al., 2012). To observe nuclei, fresh conidia or mycelia were washed with sterilized water and stained with 10 μg/mL

4′6-diamidino-2-phenylindole (DAPI, Sigma). An Olympus BX51 microscope equipped with a green fluorescent protein filter set (450- to 480-nm excitation; 515-nm emission) was used to examine the inoculated seedlings. An Olympus Fv 10i or Fluoview FV 1000 microscope with two emission-collecting windows operating simultaneously was used to generate confocal images. For AmCyan, the excitation wavelength was 405 nm, and the emission wavelength was 460–500 nm.

2.6. Generation of knockout mutants and complemented strains

SOD1 deletion mutants were generated by the split-marker recombination procedure (Catlett et al., 2003). The flanking sequences for *SOD1* are amplified as shown in Fig. S1. The resulting PCR products were transformed into PH-1 protoplasts by employing polyethyleneglycol (PEG)-mediated protoplast transformation (Proctor et al., 1995). Hygromycin B (Calbiochem, La Jolla, CA) was added to a final concentration of 400 mg/L for transformant selection. Putative gene deletion mutants were identified by genomic DNA PCR assays with primer pairs as listed in Table S1, and further confirmed by Southern blot analyses (Fig. S1 and Table S1). The probes for Southern bolt were labeled with digoxigenin using the high prime DNA labeling and detection starter kit II according to the manufacturer's protocol (Roche Diagnostics, Mannheim, Germany).

To generate complemented strains, a fragment containing *SOD1* gene and its promoter region was amplified and cloned into a vector with a neomycin resistance cassette using ClonExpress II One StepCloning Kit (vazyme) (Fig. S1). Then the constructs were transformed into protoplasts of the *SOD1* knockout mutant. The resulting transformants were screened by 400 μg/mL hygromycin B and 250 μg/mL G418 (Sigma, St. Louis, MO) simultaneously.

The primers for generating of knockout mutants and complemented strains are listed in Table S1.

2.7. Assessments of fungal growth in vitro

6-mm hyphal mass discs bored from the edge of the 3-day-old colonies on V8 agar plate were centrally attached to the 9-cm Petri dishes of V8 agar, regular potato dextrose agar (PDA), complete medium (CM) or minimal medium (MM) for 3-day growth at 25 °C in the dark. The colonies were cross-measured to compute their areas (cm^2) as growth assessment. There were three replicate plates for each experiment, and all experiments were repeated 3 times.

2.8. Stress sensitivity assays

Mycelial growth tests under to various stresses were performed as described (Jiang et al., 2012; Zheng et al., 2012). 6-mm hyphal mass discs taken from the 3-day-old Δ*sod1* mutants on V8 agar plate were centrally attached to the 9-cm Petri dishes of CM plates amended without/with 0.01%, 0.05% and 0.1% H_2O_2, 0.01% SDS, 60 μg/mL Congo red (CR), 50 μg/mL Calcoflour white (CFW) or 0.7 M NaCl. After inoculation for 3 d, the colonies were cross-measured to compute their areas (cm^2). To test for the sensitivity of conidia to H_2O_2, conidial suspension (3×10^6 conidia/mL) of the Δ*sod1* mutants was incubated in CM liquid medium with 0.003% H_2O_2 with shaking at 150 rpm. The germination percentage was examined after 4 h and 6 h, more than 200 conidia were measured for each strain.

2.9. Infection assays for virulence assessment

Florets of Bobwhite spring wheat were drop-inoculated with 10 μL fresh conidia (10^6/mL) into the floral cavity between the lemma and palea in the middle floret on the spike according to Wang et al. (2011). After inoculation, the treated florets were sprayed with water and covered with plastic bags to produce high humidity for 48 h. Three independent experiments were performed for each fungal strain and at least six wheat heads were examined. Disease was rated by the number of symptomatic spikelets at 14 day after inoculation (dai). For observing the infection progress, the florets were inoculated with AmCyanPH-1 and AmCyanΔ*sod1*, the diseased spikelets at 7 and 14 dai were dissected for microscopic analyses with Olympus Fv 10i microscope.

Three-day-old seedlings of wheat cultivar Zhongyuan 98-68 were used for the coleoptile infection assay as described (Wu et al., 2005). Three days after sowing, the top 2–3 mm of the coleoptiles were removed, and the fresh conidia (10^6/mL) were pipetted directly onto the wounded seedlings. Then the inoculated wheat coleoptiles were placed at 25 °C in a 12-h-day/12-h-night light cycle. The diseased coleoptiles photographed at 7 dai, and the lesion length was measured using ImageJ software and evaluated using Student's *t* test. More than 20 wheat seedlings per strain were evaluated in at least three independent experiments.

2.10. Analysis of trichothecene mycotoxin

Spikes of Bobwhite wheat grown in a greenhouse were drop-inoculated, and entire infected spikelet (five spikelets per strain) was harvested at 14 dai and ground to a fine powder in liquid nitrogen. DON content of each sample was assayed using Ridascreen® Fast DON ELISA kit (R-Biopharm AG, Darmstadt, Germany). DON standards included in the kit were used to produce a dose–response curve which was fitted with a rectangular hyperbola. DON concentrations in samples were calculated within the standard curve. Samples with high DON concentrations over 6 ppm were diluted with water and re-evaluated until the recorded value fell within the range of the standard curve. DON concentrations were calculated as parts per million (ppm) from fresh weight tissue of infected spikelets.

In vitro DON production was determined in culture filtrates as described (Ponts et al., 2006). Wild-type strains and the mutants were cultured in 100 mL of GYEP medium (Glucose, Yeast Extract, Peptone), and incubated for 7 d at 25 °C and 150 rpm in the dark. Cultures were done in triplicate. GYEP cultures were filtered by cheesecloth, and DON content in the filtrates was assayed as above. The filtered hyphae were desiccated in oven at 70 °C for 24 h, and weighed as fungal biomass production. DON concentrations were calculated as parts per million (ppm) from dry biomass of hyphae.

DON production in infected kernels was measured as described in Wu et al. (2015). Wheat kernels were rinsed with water overnight, and imbibed wheat kernels were further autoclaved. A 15-g aliquot in a 100 mL flask was inoculated with five 5-mm hyphal plugs of each strain from the edge of a 3-day-old colony, and then incubated at 25 °C. During incubation, the flasks were shaken once a day. After 10 day incubation, infected kernels were added into 200 mL water and homogenized, and the homogenate was filtered with 0.22 μm filter. DON content in the filtrates was measured as above. DON concentrations were calculated as parts per million (ppm) from imbibed wheat kernels.

2.11. Daminobenzide (DAB) staining

To examine the H_2O_2 accumulation of wheat coleoptile wounds, the tips (0.5–1 mm) of the seedlings were cut, the seedlings were wrapped in cotton strip which were soaked in conidia suspension (10^6/mL). The wounded coleoptiles were collected at specified timepoints for DAB staining. All samples were soaked into 1 mg/mL DAB (Sigma) solution, and covered by silver paper for 2 h at

25 °C. And then the stained samples were examined by microscope under light field.

3. Results

3.1. Five SOD genes in F. graminearum genome

Five genes were annotated as *SODs* in *F. graminearum* genome (Ma et al., 2010), including FGSG_08721, FGSG_04454, FGSG_02051, FGSG_07069 and FGSG_00576 (Table 1). FGSG_08721 encodes a protein with 76% identity to *Saccharomyces cerevisiae* SOD1 and 56% identity to *Homo sapiens* SOD1 (Garay-Arroyo et al., 2003; Awano et al., 2009), and therefore was named *SOD1*. FgSOD1 has typical Cu/Zn-binding residues (H47, H49, H64 and H121 for Cu^{2+}, and H64, H72, H81 and D84 for Zn^{2+}), the disulfide cysteines (C58 and C147), and an active site (R144) for substrate introduction (Fig. S2). The proteins encoded by FGSG_04454 and FGSG_02051 share 61% and 54% identity to SOD2 and SOD3 of *Aspergillus fumigatus*, respectively (Lambou et al., 2010), and thus they were designated *SOD2* and *SOD3* (Table 1). They have the conserved MnSOD signatures. FGSG_07069 encodes a protein which has 71% identity with *Beauveria bassiana* SOD4 (Li et al., 2015), consequently it was named *SOD4* (Table 1). FgSOD4 has two conserved regions typical for FeSODs (Fig. S2). One region is FNYASMAHNNHFFF (Fig. S3), similar to the motif (FNNAAQXWNHXFYW) critical for discrimination between FeSOD and MnSOD (Jackson and Cooper, 1998; Parker and Blake, 1988; Kim et al., 2012). The other region is FGPGFLWL, parallel to the consensus region in FeSODs of many protozoan parasites (Kim et al., 2012). FgSOD2 and FgSOD4 have predicted mitochondria targeting signal sequences (Fig. S3). FGSG_00576 encodes a protein shares 45% identity to *B. bassiana* SOD5 (Li et al., 2015), accordingly, we named this protein SOD5. FgSOD5 possesses the copper binding histidines (H87, H89, H105, and H170), the disulfide cysteines (C100 and C179), and the active arginine (R176) as SOD1 does, but it lacks two of four zinc binding histidines and 17 residues of the electrostatic loop (Fig. S2). SOD5-like proteins were found throughout Ascomycota and Basidiomycota fungi, each retaining the SOD1-like copper site and disulfide but missing zinc binding and the electrostatic loop region (Gleason et al., 2014). FgSOD5 has a N-terminal signal peptide, and is most likely an extracellular CuSOD.

Next, we performed the phylogeny analysis of FgSODs with other typical SODs in eukaryotes. The phylogenetic tree showed that these FgSODs occupy distinct and divergent branches, falling into five clades (Fig. S4). FgSOD1 clustered with SOD1 proteins from human, yeast and filamentous fungi into a clade, a cytoplasmic Cu-Zn SOD1 group.

Table 1
SOD genes in *F. graminearum*.

Gene ID	Gene name	Type	Putative subcellular localization
FGSG_08721	*SOD1*	Cu-Zn SOD	Cytoplasmic
FGSG_04454	*SOD2*	Mn SOD	Mitochondrial
FGSG_02051	*SOD3*	Mn SOD	Cytoplasmic
FGSG_07069	*SOD4*	Fe SOD	Mitochondrial
FGSG_00576	*SOD5*	Cu SOD	Secreted/extracellular space

3.2. SOD genes are differentially expressed, and SOD1 is strongly expressed in vitro culture and in planta

To understand biological functions of these *SOD* genes, we compared their expression profiles during vegetative and invasive growth based on published microarray data from *F. graminearum* conidial germination and infection series in wheat coleoptiles, heads and crowns (Seong et al., 2008; Stephens et al., 2008; Lysoe et al., 2011; Zhang et al., 2012). *SOD1* is highly expressed in fresh conidia, conidia with emerging germ tube and elongating conidia as well as branching hyphae compared with other *SOD* genes (Fig. 1). *SOD1* is also highly expressed during wheat coleoptile and head infection as well as crown rot disease (Fig. 1). *SOD3* was detected to be strongly expressed in branching hyphae and invasive hyphae at biotrophic stage during wheat head infection (Fig. 1). The other *SOD* genes showed no obvious change in expression during vegetative growth and infection (Fig. 1). *SOD2* is expressed at medium level while *SOD4* and *SOD5* are weakly expressed *in vitro* culture and plant infection (Fig. 1).

Of five *SOD* genes, *SOD1* is the highest expression level during all vegetative developmental stages and infection processes of *F. graminearum* based on microarray data. The expression of *SOD1* in spore, hyphae and during wheat coleoptile infection was verified by quantitative PCR after reverse transcription. Quantitative PCR results were congruous with that of microarray data (Fig. S5). We therefore prioritized SOD1 for functional analysis.

3.3. SOD1 localizes in cytoplasm with a superoxide dismutase activity

SOD1 was predicted to be localized in cytoplasm (Table 1). To verify this, we constructed *F. graminearum* strain constitutively expressing SOD1-mRFP fusion protein. During *in vitro* culture, RFP signals were observed in cytosol of growing hyphae region close to tip, and in the cytoplasmic aggregations in hyphal regions far from growing tip and in conidia (Fig. 2A). These aggregations are distinct from DAPI-stained nuclei (Fig. 2A), but similar to distri-

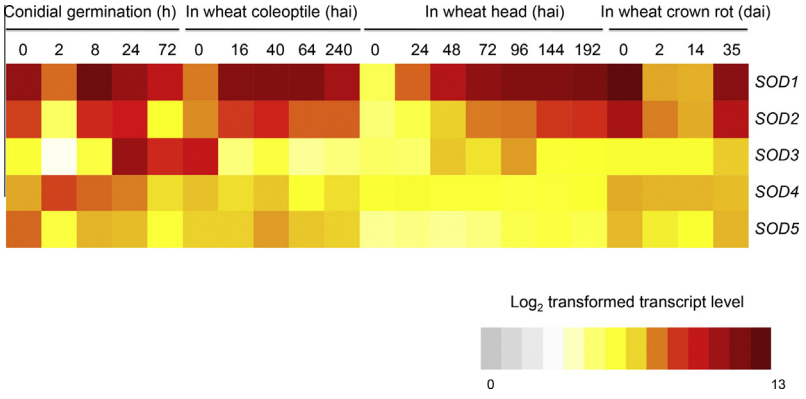

Fig. 1. Heat maps showing the expression patterns of five *SOD* genes *in vitro* growth and *in planta*. Microarray data on *SOD* genes during conidium development (Seong et al., 2008), wheat coleoptile infection (Zhang et al., 2012), wheat head blight (Lysoe et al., 2011) and crown rot disease (Stephens et al., 2008) were analyzed. hai, hours after inoculation; dai, days after inoculation.

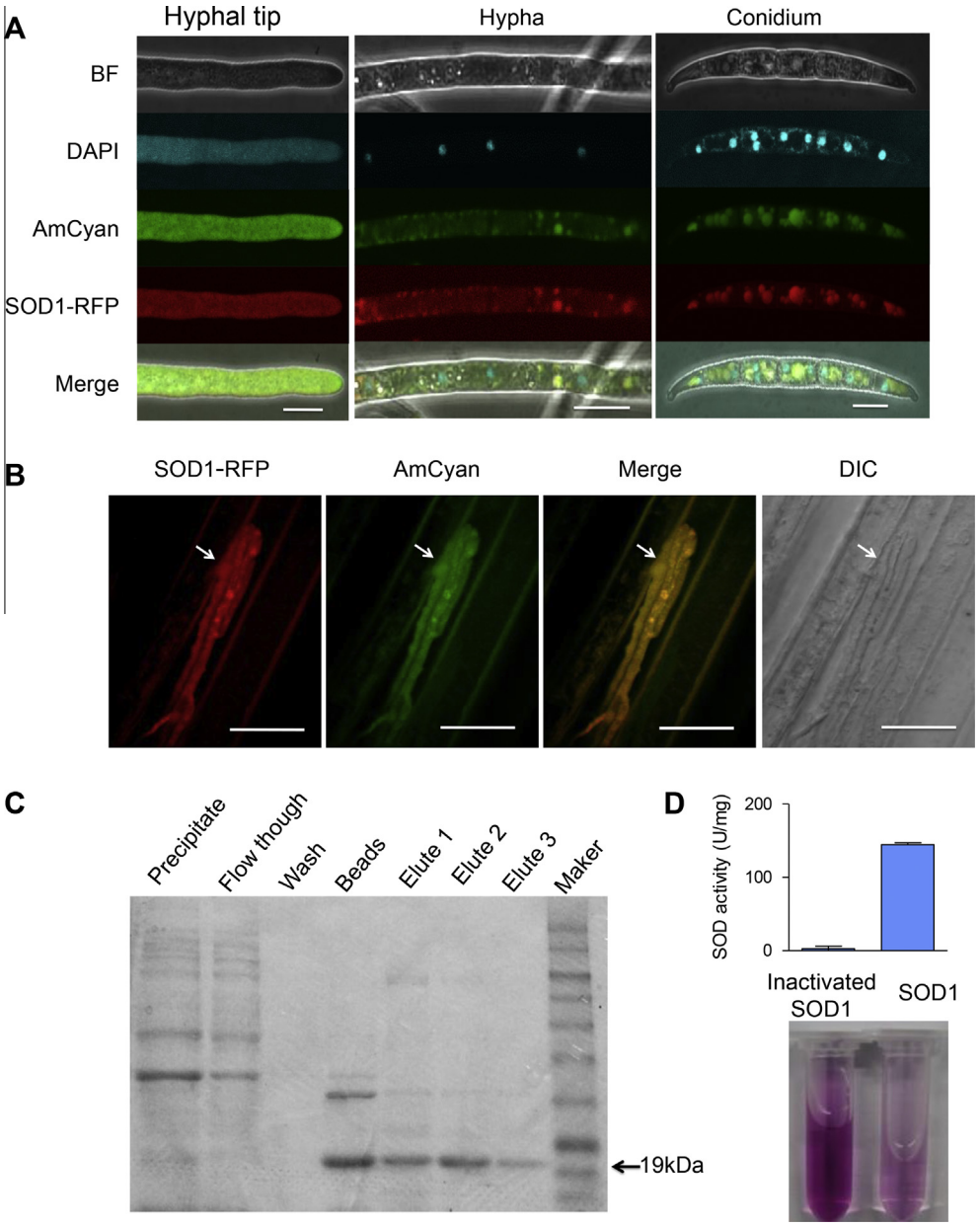

Fig. 2. SOD1 localizes in cytoplasm and has superoxide dismutase activity. (A and B) Subcellular localization of SOD1-RFP fusion proteins in *F. graminearum* that cultured *in vitro* (A) and during infection of wheat coleoptile at 40 hai (B). Hyphae and conidia of the SOD1-mRFP and AmCyan co-expressed transformants were stained with DAPI before being examined by confocal laser scanning microscope. Bar = 20 μm. White arrows point to the fungal hyphae. (C) SDS-PAGE of purified SOD1 from each step of the purification procedure. (D) The Cu-Zn SOD1 enzyme activity was measured. Error bars indicate standard errors derived from three independent experiments.

bution of the cytoplasmic AmCyan as reported in a previous study (Zhang et al., 2012). During infection of wheat coleoptile, SOD1-mRFP fusion protein was also observed in cytoplasm of invasive hyphae growing inside wheat coleoptile cells (Fig. 2B).

To verify the biochemical activity, we expressed *SOD1* in *E. coli*. The size of purified recombinant SOD1 was consistent with the prediction (Fig. 2C). Using a Cu/Zn SOD activity assay kit, we showed that the purified SOD1 inhibited xanthine oxidation, while a heat-inactivated SOD1 did not (Fig. 2D). Therefore SOD1 had the superoxide dismutase activity *in vitro*.

3.4. Targeted gene deletion of SOD1 attenuates hyphal and germ tube growth

To explore the biological function of SOD1 in *F. graminearum*, a split-marker approach was adopted to generate a mutant lacking *SOD1* gene (Catlett et al., 2003). A deletion allele was created by replacement of the *SOD1* coding region with a constitutively-expressed hygromycin resistance gene (*HPH*) (Fig. S1A, B and C). Three independent Δ*sod1* mutants (designated as M1, M2 and M3) were constructed and verified by genomic DNA PCR and Southern blot hybridization (Fig. S1E and F). These mutants have a correct and unique integration event of corresponding resistance gene in the expected locus. The Δ*sod1* mutants were found to have slightly smaller colony size than the wild-type strain PH-1 on V8 plates after incubation for 3 days, indicating that the mutation of *SOD1* lead to small reduction in hyphal growth speed (Fig. 3A). We also measured the colony areas of Δ*sod1* mutants on PDA, CM and MM for 3 days. The colony areas of Δ*sod1* were about 20% smaller than that of wild type (Fig. 3B). Hence the Δ*sod1* mutants showed reduced growth in all tested media. For complementation assays, the fragment containing the Δ*sod1* and its pro-

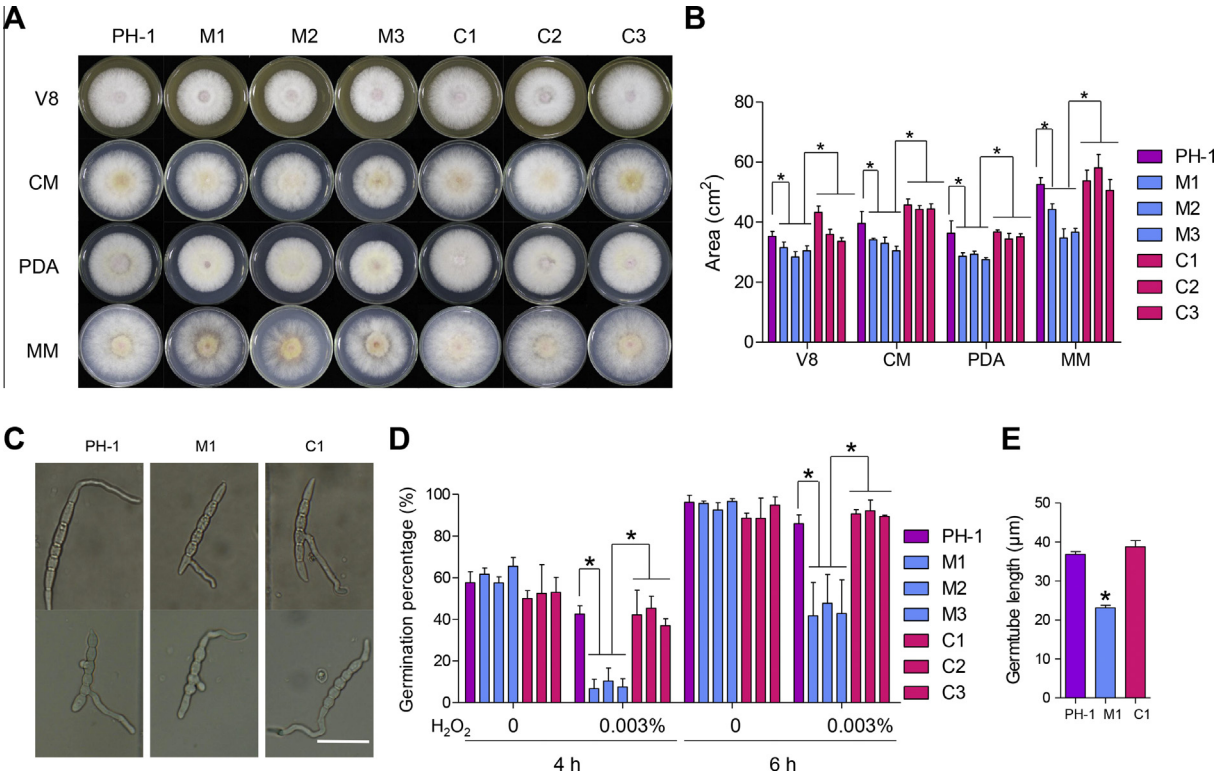

Fig. 3. Deletion of *SOD1* attenuates fungal growth *in vitro*. (A) Colonies of PH-1, Δ*sod1* mutants and complemented strains cultured on V8, CM, PDA and MM plates at 25 °C for 3 days. (B) Measurements of colony areas of the indicated strains. Error bars represent the standard error from three independent experiments and asterisks indicate statistically significant differences (Student's *t* test, $P < 0.05$). (C) Conidial germination of PH-1, the *Δsod1* mutants and the complemented strains was examined after 6 h culture in liquid CM. (D) Measurements of germination percentages. (E) Germ tube length were measured after 6 h in liquid CM. More than 200 conidia were scored for each strain. Asterisks indicate statistically significant differences (Student's *t* test, $P < 0.05$).

moter region as well as neomycin resistance gene was transformed into the Δ*sod1* mutants (Fig. S1D). The complemented strains (C1, C2 and C3) restored the growth of the Δ*sod1* mutants (Fig. 3).

There is no recognizable difference in the morphology of conidia and hyphae of Δ*sod1* mutants compared with wild-type strain (Fig. S6). When incubated in liquid CM, conidia of the Δ*sod1* mutants were able to germinate from the end and middle compartments, just like the wild type (Fig. 3C). In addition, there is no significant difference in conidial germination percentage between the Δ*sod1* mutants and the wild type when measured after 4 or 6 h culture (Fig. 3D). But the germ tubes of the Δ*sod1* mutant were about 40% shorter than those of wild type, when measured after 6 h culture (Fig. 3E). The defect of the Δ*sod1* mutant in germ tube growth was consistent with its reduced hyphal growth speed. These results indicate that deletion of *SOD1* affects vegetative growth of *F. graminearum*.

3.5. Deletion of SOD1 increases the sensitivity to intracellular superoxide radicals

Considering that SOD1 was localized in cytoplasm, we detected the sensitivity of Δ*sod1* mutants to menadione that is known to generate intracellular superoxide free radicals (Kawamura et al., 2006). The mutants were grown on CM plates containing various concentrations of menadione. Compared with the wild-type strain, the mutants formed the remarkable reduced size of colones with 30 or 60 μM menadione (Fig. 4A). Colony areas of wild-type strain grown with 30 μM menadione were about 60% of those grown without menadione, but colony areas of Δ*sod1* mutants grown with 30 μM menadione were only about 20% of those mutants grown without menadione (Fig. 4B). Similarly, colony areas of wild-type strain grown with 60 μM menadione were about 35% of those grown without menadione, while colony areas of Δ*sod1* mutants grown with 60 μM menadione were only about 10% of those grown without menadione (Fig. 4B). These results indicated that the Δ*sod1* mutants were hypersensitive to menadione. All complemented transformant strains showed the sensitivity to menadione similar to the wild-type strain (Fig. 4). These results showed that SOD1 in *F. graminearum* is responsible for scavenging intracellular superoxide radicals.

3.6. Deletion of SOD1 did not increase hyphal sensitivity to several extracellular stresses

In the presence of 0.01%, 0.05% or 0.1% H_2O_2 during *in vitro* culture, the 3-day colony areas of the wild-type strains were reduced to about 85%, 55% and 35% of those grown without H_2O_2, respectively (Fig. S7A); and the colony areas of Δ*sod1* mutants were about 100%, 75% and 45% of the mutants grown without H_2O_2, respectively (Fig. S7A). The results indicate that the Δ*sod1* mutants are not more sensitive to exogenous oxidative stress than the wild-type. Similar result was observed for the complemented strains (Fig. S7). These data indicate that SOD1 may not responsible for protecting against extracellular oxidative stress in *F. graminearum* during hyphal growth.

It has been demonstrated in budding yeast that Cu/Zn SOD plays a general role in the maintenance of fungal cell wall integrity (Liu et al., 2010). We investigated the effect of cell wall-perturbing agents, including Calcoflour white (CFW) and Congo red (CR), on hyphal growth of the Δ*sod1* mutants. In the presence of 50 μg/mL CFW or 60 mg/L CR, hyphal growth of Δ*sod1* mutants is comparable to that of the wild type and the complemented strains (Fig. S7C). These results indicate that SOD1 in *F. graminearum*

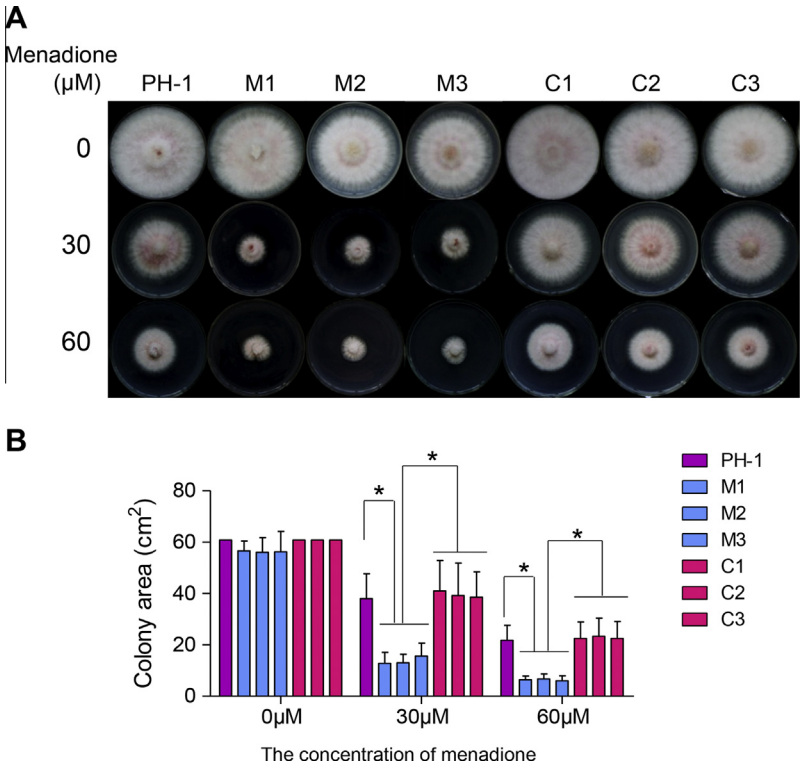

Fig. 4. The Δ*sod1* mutants showed increased sensitivity to intracellular superoxide radicals. (A) The wild type, *Δsod1* mutants and the complemented strains were cultured on CM plates containing different concentration of menadione for 4 days. (B) Measurements of the colony areas of the indicated strains. Error bars represent the standard error from three independent experiments and asterisks indicate statistically significant differences (Student's *t* test, $P < 0.05$).

may not play important roles in the maintenance of cell wall integrity.

We also examined the effect of membrane stress and hyperosmotic stress on the Δ*sod1* mutants. The Δ*sod1* mutants showed comparable sensitivity to membrane stress and hyperosmotic shock with the wild-type and the complemented strains in the presence of 0.01% SDS and 0.7 M NaCl (Fig. S7C), suggesting that deletion of *SOD1* does not affect the responses to membrane and osmotic stresses.

3.7. Deletion of SOD1 delayed conidial germination under exogenous H_2O_2

Since the Δ*sod1* mutants have no defects for oxidative stress and other general stresses in hyphal growth, we next examined the effect of the oxidative stress on conidial germination. Without supplement of H_2O_2, the conidial germination percentages (measured at 4 h and 6 h) of the mutants and the wild type were similar. With supplemented with 0.003% H_2O_2, after 4 h of culturing, about 40% of wild-type conidia germinated, while only about 10% of Δ*sod1* conidia germinated; After 6 h, about 90% of wild-type conidia germinated, while only about 40% of mutant conidia germinated (Fig. 3D). With 0.003% H_2O_2, the conidial germination percentage of the Δ*sod1* mutants at 6 h was similar to that of wild type at 4 h, indicating deletion of SOD1 delayed conidial germination. The complemented strains showed similar conidial germination percentage with the wild-type strain (Fig. 3D). Therefore, SOD1 is important in response to oxidative stress during conidial germination.

3.8. Deletion of SOD1 resulted in reduced virulence in wheat floret infection

To investigate the role of SOD1 in *F. graminearum* virulence, we performed wheat floret infection assay. The conidial suspension of Δ*sod1* mutants were inoculated on wheat spikelets between lemma and palea, and the symptoms were assessed at 14 days after inoculation (dai). All the three independent lines of Δ*sod1* mutants caused discolor symptom in the inoculated wheat spikelets, but none of them was able to spread to surrounding spikelets (Fig. 5A). It is clear that the virulence of Δ*sod1* mutants in wheat head infection were severely reduced than wild-type strain (Fig. 5B). The complemented strains showed similar virulence to the wild-type strain (Fig. 5A and B). Therefore, SOD1 is important for virulence in wheat floret infection.

To track the infection progress, we transformed the AmCyan fluorescent protein construct into the Δ*sod1* mutant, and inoculated the wheat florets with conidial suspension of AmCyanΔ*sod1* and AmCyanPH-1. At 7 dai, the AmCyanΔ*sod1*-inoculated spikelet showed minimal disease symptom while the AmCyanPH-1-inoculated spikelet had typical scab symptom (Fig. 5C). Microscopic analysis showed that in the AmCyanPH-1-inoculated spikelet, ample hyphae were seen in lamma and palea, and some hyphae penetrated into rachis below the inoculated spikelet; however, in the Δ*sod1*-inoculated spikelets, only a few hyphae were seen in lamma and palea, and no hypha was visible in rachis (Figs. 5C and S8). At 14 dai, in the AmCyanPH-1-inoculated spike, symptoms eventually spread up and progressed down the neighboring spikelets from the inoculated spikelet, the diseased spikelet was colonized by aerial hyphae and the advancing hyphal front was visible in the rachis of the distal diseased spikelet (Fig. 5C). In the AmCyanΔ*sod1*-inoculated wheat spike at 14 dai, only the inoculated spikelet exhibited head blight symptom, and the infection hyphal front just reached the upper part of the rachis of the inoculated spikelet, still no hypha was visible in the lower part of the rachis (Fig. 5C). These results show that the Δ*sod1* mutant could not grow through the rachis during wheat floret infection.

We also examined the infection of the Δ*sod1* mutant on wheat coleoptile. The wounded coleoptiles were inoculated with conidial

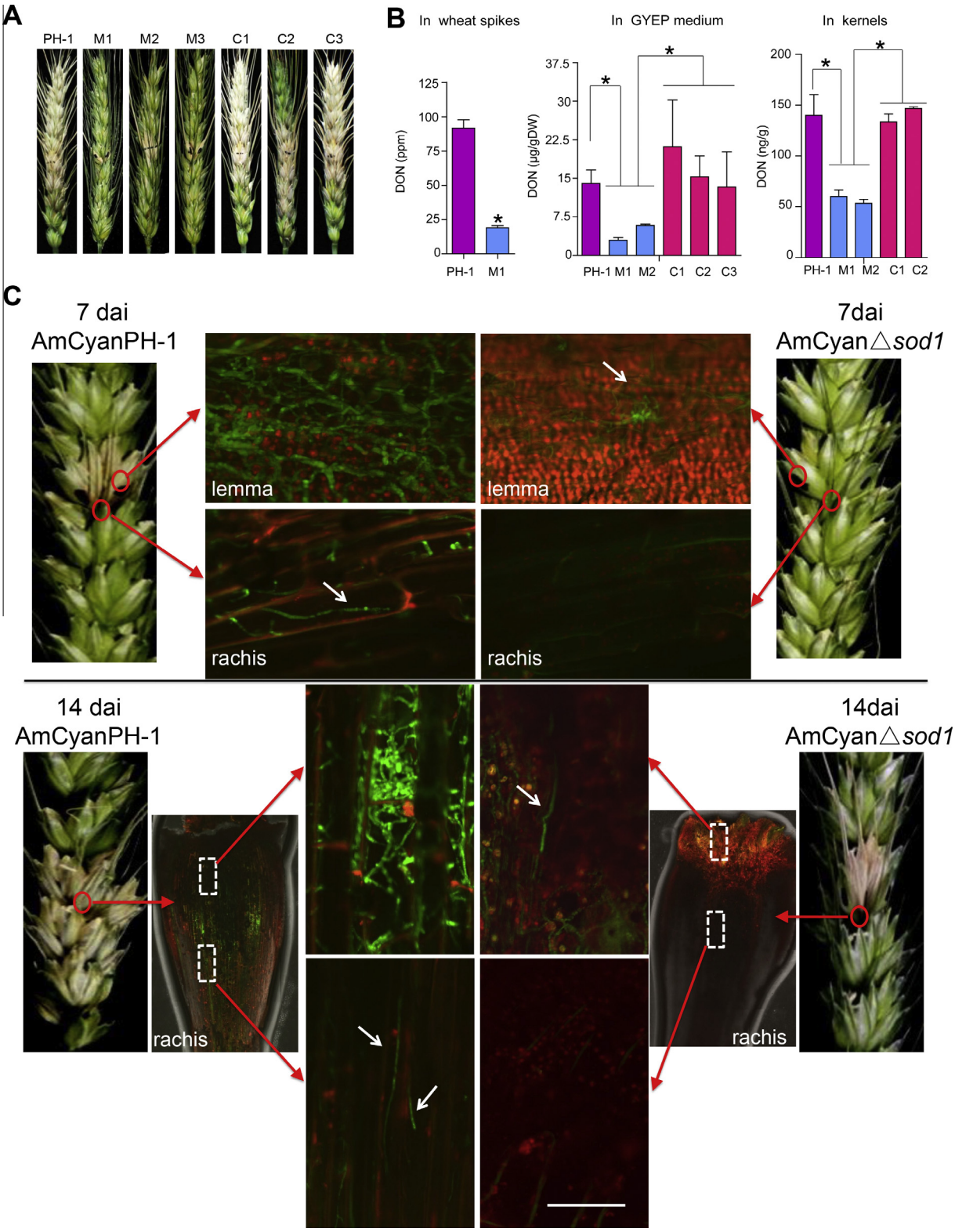

Fig. 5. SOD1 is required for virulence in wheat head infection. (A) Representative pictures of wheat spikes inoculated with indicated strains at 14 days after inoculation (dai). Black dots mark the inoculated spikelets. (B) Measurements of DON contents. Asterisks indicate statistically significant differences (Student's *t* test, $P < 0.05$). (C) Representative confocal laser microscopy images of AmCyanPH-1 and AmCyan*Δsod1* at 7 dai and 14 dai. White arrows point to hyphae. Scale bar = 100 μm.

suspension of the *Δsod1* mutants with AmCyan fluorescent protein construct. Microscopic analyses showed that the hyphal extension of the AmCyan*Δsod1* mutants inside coleoptile cells was slower compared with the wild-type and complemented strains at 16 hai (Fig. S9C and D). However, the difference in hyphal extension distance from wounding sites between the *Δsod1* mutants and the wild-type or complemented strains was not significant at 40 hai (Fig. S9D). We further measured the lesion size in infected coleoptiles at 7 dai, and found that the lesion size of the *Δsod1* mutants was similar to that produced by the wild type (Fig. S9A

and B). These results indicate that the Δ*sod1* strains have small defects in virulence associated with early stages of infection, resulting in the delay of hyphal progression into coleoptile cells.

3.9. DON production is impaired in the Δsod1 mutant

The mycotoxin DON is a known virulence factor of *F. graminearum* during wheat head blight infection (Proctor et al., 1995; Harris et al., 1999). To further explore the reason for virulence reduction of the Δ*sod1* mutant, we measured DON production in diseased wheat spikes at 14 dai. Whereas DON content in PH-1-infected spikelets exceeded 90 ppm, DON content in the Δ*sod1*-infected spikes was less than 20 ppm (Fig. 5B). DON content in the mutant infected spike is less than one-fourth of that in wild type-infected ones. This result revealed that DON biosynthesis in the Δ*sod1* mutant during infection of wheat florets was compromised.

We also detected that DON production of the Δ*sod1* mutants in DON-inducing medium or in autoclaved wheat kernels was lower than that of wild type (Fig. 5B). Complemented strains produced more DON than mutants in the above conditions. Therefore, we conclude that SOD1 deletion caused the reduction of DON production capability of *F. graminearum*.

4. Discussion

In this study, we identified five distinct *SOD* genes from *F. graminearum* genome. These SODs fall into different types, localize different cellular compartment and had different expression patterns. Similar to other plant and human pathogenic fungi (Lambou et al., 2010; Li et al., 2015), multiple SOD proteins may constitute complex superoxide-scavenging system for confronting endogenous and exogenous stresses in *F. graminearum*.

Most impressively, deletion of a cytoplasmic Cu-Zn SOD1 in *F. graminearum* significantly reduced its virulence in wheat head blight infection (Fig. 5). The Δ*sod1* mutant failed to pass through rachis to infect spikelets other than the inoculated one. This mutant phenotype in wheat floret infection is more severe than its reduction in hyphal growth *in vitro*. The reasons may include the reduction of DON production in Δ*sod1* mutants (Fig. 5B). The trichothecene mycotoxin DON, is an important virulence factor for *F. graminearum* infection of wheat, as DON biosynthesis deficient mutants typically have attenuated disease symptoms and DON promotes the spreading of the pathogen (Proctor et al., 1995). It has been reported that DON production allows *F. graminearum* to pass through rachis and escape host cell wall thickening in wheat head blight infection (Jansen et al., 2005).

To a certain degree, this can explain to the fact that the Δ*sod1* mutant was slightly reduced in hyphal growth but strongly reduced its virulence on wheat florets. Furthermore, the role of DON in infection of different hosts can be different. For example, DON is not a virulence factor for barley head infection, though its production is detected during barley head blight infection (Jansen et al., 2005). Previous studies showed that no DON biosynthesis genes are induced during wheat coleoptile infection (Zhang et al., 2012), indicating that no DON production during wheat coleoptile infection. This may help to explain that, unlike in wheat head blight infection, the Δ*sod1* mutant had similar virulence to the wild type on wheat coleoptiles. While the *in vitro* analysis detected a significant reduction in hyphal growth caused by *SOD1* deletion, it is possible that such effect is overwhelmed by the large variation in fungal growth during plant infection, which is caused by un-synchronized growth, and other complex factors *in vivo*.

Then how to explain that the infection progress of the Δ*sod1* mutant on wheat coleoptiles was affected in early infection stage (16 hai)? We found that large amount of ROS accumulation in the wounding sites of wheat coleoptiles, particularly after *F. graminearum* inoculation, compared with intact wheat coleoptiles (Fig. S10). Also, the Δ*sod1* mutants conidial germination were about 2 h delayed than the wild type under exogenous H_2O_2 (Fig. 3D), while hyphal growth reduction under exogenous H_2O_2 of Δ*sod1* mutants were similar to the wild type (Fig. S7A). Therefore, ROS in wounding sites may delay conidial germination of Δ*sod1* mutants, thereby leading to the outcome that the hyphal extension of the Δ*sod1* mutants inside coleoptile cells was slower than the wild-type at early infection stage. Later on the hyphal growth were similar between the mutants and wild-type strains, therefore difference in infection distance between the Δ*sod1* mutants and the wild-type at 40 hai was not significant.

The SOD1 is well conserved throughout evolution and found in all organisms, including bacteria, fungi and mammalian (Fridovich, 1995). Disruption of cytoplasmic Cu-Zn SOD1 in *F. graminearum* caused a reduced hyphal and germ tube growth, increased the sensitivity to intracellular superoxide anion, decreased DON production and reduced pathogenicity on wheat head blight infection. Consistent with pleiotropic phenotypes of *SOD1* mutation in *F. graminearum*, SOD1 homologs in other fungi also play multiple roles. Mutation of a Cu-Zn *SOD1* from *Sclerotinia sclerotiorum* reduces hyphal growth, oxalate production as well as virulence on both tomato and tobacco plants, and also displays developmental defects in sclerotia formation (Veluchamy et al., 2012). In filamentous entomopathogen *B. bassiana*, the Δ*sod1* mutant showed a significant delay of the conidiation and conidial germination, more sensitive to menadione, H_2O_2 and UV-A/UV-B irradiations and less virulent to *Galleria mellonella* larvae (Li et al., 2015). In human fungal pathogen *Candida albicans*, the Cu-Zn SOD1-defcient strain exhibited slower growth in minimal medium and more sensitive to menadione, increased susceptibility to macrophage attack and had attenuated virulence in mice (Hwang et al., 2002). In *A. fumigatus*, the Δ*sod1* mutant showed a growth inhibition at high temperature, a hypersensitivity to menadione and an increased sensitivity to killing by alveolar macrophage of immunocompetent mice (Lambou et al., 2010).

F. graminearum lacking *SOD1* exhibited no more sensitivity to extracellular oxidative stress. The function of SOD1 in *F. graminearum* support the notion that Cu-ZnSOD primarily scavenges cytosolic ROS by catalyze the dismutation of superoxide ion to hydrogen peroxide and oxygen molecule, thus protecting against intracellular superoxide stress (Zelko et al., 2002). The deletion mutant of *SOD1* of *S. cerevisiae* is more sensitive to cell wall-perturbing agents (Liu et al., 2010). However, the Δ*sod1* mutant of *F. graminearum* had no alteration in sensitivity to cell wall-perturbing agents, suggesting that SOD1 is not required for the maintenance of fungal cell wall integrity in *F. graminearum*. SOD1 in *Cryptococcus neoformans* was also found to be associated with hyperosmotic stress response (Narasipura et al., 2005), but the Δ*sod1* mutant of *F. graminearum* had no change in cellular responses to high osmolarity. The responses of the Δ*sod1* mutant to extracellular stresses further revealed that SOD1 is responsible for destroying the radicals that are normally produced within cells rather than generated from extracellular environmental stresses. The slightly reduced growth of the Δ*sod1* mutant is most likely to stem from its impaired ability to alleviate superoxide stress arising from altered metabolism rather than insufficient scavenging of exogenous superoxide radicals. In addition, we could not rule out the possibility that another cytoplasmic MnSOD protein SOD3 may partially compensate for the function of SOD1 in *F. graminearum*, thereby leading to weak growth defect in the Δ*sod1* mutant.

It is also interesting to find that the SOD1 deletion delayed conidial germination under exogenous H_2O_2, though SOD1 is mainly scavenging intracellular superoxide anion. H_2O_2 is membrane-permeable, and polar localized ROS in the cell play a role in signaling during conidial germination (Gessler et al., 2007; Veal and Day, 2011). Therefore exogenous H_2O_2 may interfere with localized ROS signaling, in wild type, SOD1 possibly produces more H_2O_2 locally to alleviate the exogenous H_2O_2 interference, while in the mutant the interference became severe. The complicated relation between *in vitro* phenotype and infection phenotype of *F. graminearum* suggests that host infection outcome tightly linked to the fungal growth and development.

This study showed that intracellular oxidative stress is associated with DON production in *F. graminearum*. Actually, accumulating evidence has demonstrated that DON biosynthesis and response to oxidative stress are intertwined in *F. graminearum*. Two previous results indicate that oxidative stress with H_2O_2 could be a prerequisite for DON biosynthesis (Ponts et al., 2006, 2007). The transcription factor *FgAP1* that activates the transcription of antioxidant enzymes was shown to regulate stress response and DON synthesis (Montibus et al., 2013). Similarly, the transcription regulator FgSKN7 appears to be involved in oxidative stress response, as well as DON biosynthesis (Jiang et al., 2015). A recent study demonstrated that a glycogen synthase kinase GSK3 is essential for both virulence and DON production, and to be upregulated upon oxidative stress by H_2O_2 (Qin et al., 2015). These data together with our result strongly suggest that mycotoxin DON biosynthesis and response to oxidative stress are interconnected. Therefore, a future research topic is to explore how the SOD-based ROS scavenging system is linked to DON production in *F. graminearum*.

Acknowledgments

We thank Dr. Xuan Li for advice on statistical analysis. This work was supported by the Chinese Academy of Sciences (Grant XDB11020500) and the Ministry of Agriculture of China (2016ZX08009-003).

Appendix A. Supplementary material

Supplementary data associated with this article can be found, in the online version, at http://dx.doi.org/10.1016/j.fgb.2016.03.006.

References

Abba, S., Khouja, H.R., Martino, E., Archer, D.B., Perotto, S., 2009. SOD1-targeted gene disruption in the ericoid mycorrhizal fungus *Oidiodendron maius* reduces conidiation and the capacity for mycorrhization. Mol. Plant Microbe Interact. 22, 1412–1421.

Aguirre, J., Rios-Momberg, M., Hewitt, D., Hansberg, W., 2005. Reactive oxygen species and development in microbial eukaryotes. Trends Microbiol. 13, 111–118.

Apel, K., Hirt, H., 2004. Reactive oxygen species: metabolism, oxidative stress, and signal transduction. Annu. Rev. Plant Biol. 55, 373–399.

Awano, T., Johnson, G.S., Wade, C.M., Katz, M.L., Johnson, G.C., Taylor, J.F., et al., 2009. Genome-wide association analysis reveals a *SOD1* mutation in canine degenerative myelopathy that resembles amyotrophic lateral sclerosis. Proc. Natl. Acad. Sci. U.S.A. 106, 2794–2799.

Catlett, N., Lee, B.-N., Yoder, O., Turgeon, B.G., 2003. Split-marker recombination for efficient targeted deletion of fungal genes. Fungal Genet. Newsl. 50, 9–11.

Dal Bello, G., Monaco, C., Simon, M., 2002. Biological control of seedling blight of wheat caused by *Fusarium graminearum* with beneficial rhizosphere microorganisms. World J. Microbiol. Biotechnol. 18, 627–636.

Fridovich, I., 1995. Superoxide radical and superoxide dismutases. Annu. Rev. Biochem. 64, 97–112.

Garay-Arroyo, A., Lledias, F., Hansberg, W., Covarrubias, A.A., 2003. Cu,Zn-superoxide dismutase of *Saccharomyces cerevisiae* is required for resistance to hyperosmosis. FEBS Lett. 539, 68–72.

Gessler, N.N., Aver'yanov, A.A., Belozerskaya, T.A., 2007. Reactive oxygen species in regulation of fungal development. Biochemistry (Moscow) 72, 1091–1109.

Gleason, J.E., Galaleldeen, A., Peterson, R.L., Taylor, A.B., Holloway, S.P., Waninger-Saroni, J., et al., 2014. *Candida albicans* SOD5 represents the prototype of an unprecedented class of Cu-only superoxide dismutases required for pathogen defense. Proc. Natl. Acad. Sci. U.S.A. 111, 5866–5871.

Goswami, R.S., Kistler, H.C., 2004. Heading for disaster: *Fusarium graminearum* on cereal crops. Mol. Plant Pathol. 5, 515–525.

Halliwell, B., Gutteridge, J.M., 2015. Free Radicals in Biology and Medicine, fifth ed. Oxford University Press, New York.

Harris, L., Desjardins, A.E., Plattner, R., Nicholson, P., Butler, G., Young, J., et al., 1999. Possible role of trichothecene mycotoxins in virulence of *Fusarium graminearum* on maize. Plant Dis. 83, 954–960.

Hasan, R., Leroy, C., Isnard, A.D., Labarre, J., Boy-Marcotte, E., Toledano, M.B., 2002. The control of the yeast H_2O_2 response by the Msn2/4 transcription factors. Mol. Microbiol. 45, 233–241.

Heindorf, M., Kadari, M., Heider, C., Skiebe, E., Wilharm, G., 2014. Impact of *Acinetobacter baumannii* superoxide dismutase on motility, virulence, oxidative stress resistance and susceptibility to antibiotics. PLoS ONE 9, e101033.

Hwang, C.S., Baek, Y.U., Yim, H.S., Kang, S.O., 2003. Protective roles of mitochondrial manganese-containing superoxide dismutase against various stresses in *Candida albicans*. Yeast 20, 929–941.

Hwang, C.S., Rhie, G.E., Oh, J.H., Huh, W.K., Yim, H.S., Kang, S.O., 2002. Copper- and zinc-containing superoxide dismutase (Cu/ZnSOD) is required for the protection of *Candida albicans* against oxidative stresses and the expression of its full virulence. Microbiology 148, 3705–3713.

Jackson, S.M., Cooper, J.B., 1998. An analysis of structural similarity in the iron and manganese superoxide dismutases based on known structures and sequences. Biometals 11, 159–173.

Jansen, C., von Wettstein, D., Schafer, W., Kogel, K.H., Felk, A., Maier, F.J., 2005. Infection patterns in barley and wheat spikes inoculated with wild-type and trichodiene synthase gene disrupted *Fusarium graminearum*. Proc. Natl. Acad. Sci. U.S.A. 102, 16892–16897.

Jiang, C., Zhang, S., Zhang, Q., Tao, Y., Wang, C., Xu, J.R., 2015. FgSKN7 and FgATF1 have overlapping functions in ascosporogenesis, pathogenesis and stress responses in *Fusarium graminearum*. Environ. Microbiol. 17, 1245–1260.

Jiang, J., Yun, Y., Liu, Y., Ma, Z., 2012. FgVELB is associated with vegetative differentiation, secondary metabolism and virulence in *Fusarium graminearum*. Fungal Genet. Biol. 49, 653–662.

Kawamura, F., Hirashima, N., Furuno, T., Nakanishi, M., 2006. Effects of 2-methyl-1,4-naphtoquinone (menadione) on cellular signaling in RBL-2H3 cells. Biol. Pharm. Bull. 29, 605–607.

Kazan, K., Gardiner, D.M., Manners, J.M., 2012. On the trail of a cereal killer: recent advances in *Fusarium graminearum* pathogenomics and host resistance. Mol. Plant Pathol. 13, 399–413.

Kim, J.Y., Na, B.K., Song, K.J., Park, M.H., Park, Y.K., Kim, T.S., 2012. Functional expression and characterization of an iron-containing superoxide dismutase of *Acanthamoeba castellanii*. Parasitol. Res. 111, 1673–1682.

Kim, K.H., Willger, S.D., Park, S.W., Puttikamonkul, S., Grahl, N., Cho, Y., et al., 2009. TmpL, a transmembrane protein required for intracellular redox homeostasis and virulence in a plant and an animal fungal pathogen. PLoS Pathog. 5, e1000653.

Lambou, K., Lamarre, C., Beau, R., Dufour, N., Latge, J.P., 2010. Functional analysis of the superoxide dismutase family in *Aspergillus fumigatus*. Mol. Microbiol. 75, 910–923.

Li, F., Shi, H.Q., Ying, S.H., Feng, M.G., 2015. Distinct contributions of one Fe- and two Cu/Zn-cofactored superoxide dismutases to antioxidation, UV tolerance and virulence of *Beauveria bassiana*. Fungal Genet. Biol. 81, 160–171.

Liu, X., Zhang, X., Zhang, Z., 2010. Cu,Zn-superoxide dismutase is required for cell wall structure and for tolerance to cell wall-perturbing agents in *Saccharomyces cerevisiae*. FEBS Lett. 584, 1245–1250.

Lynch, M., Kuramitsu, H., 2000. Expression and role of superoxide dismutases (SOD) in pathogenic bacteria. Microbes Infect. 2, 1245–1255.

Lysoe, E., Seong, K.Y., Kistler, H.C., 2011. The transcriptome of *Fusarium graminearum* during the infection of wheat. Mol. Plant Microbe Interact. 24, 995–1000.

Ma, L.J., van der Does, H.C., Borkovich, K.A., Coleman, J.J., Daboussi, M.J., Di Pietro, A., et al., 2010. Comparative genomics reveals mobile pathogenicity chromosomes in *Fusarium*. Nature 464, 367–373.

Montibus, M., Ducos, C., Bonnin-Verdal, M.N., Bormann, J., Ponts, N., Richard-Forget, F., et al., 2013. The bZIP transcription factor Fgap1 mediates oxidative stress response and trichothecene biosynthesis but not virulence in *Fusarium graminearum*. PLoS ONE 8, e83377.

Narasipura, S.D., Chaturvedi, V., Chaturvedi, S., 2005. Characterization of *Cryptococcus neoformans* variety gattii SOD2 reveals distinct roles of the two superoxide dismutases in fungal biology and virulence. Mol. Microbiol. 55, 1782–1800.

Parker, M.W., Blake, C.C., 1988. Crystal structure of manganese superoxide dismutase from *Bacillus stearothermophilus* at 2.4 A resolution. J. Mol. Biol. 199, 649–661.

Ponts, N., Pinson-Gadais, L., Barreau, C., Richard-Forget, F., Ouellet, T., 2007. Exogenous H_2O_2 and catalase treatments interfere with Tri genes expression in liquid cultures of *Fusarium graminearum*. FEBS Lett. 581, 443–447.

Ponts, N., Pinson-Gadais, L., Verdal-Bonnin, M.N., Barreau, C., Richard-Forget, F., 2006. Accumulation of deoxynivalenol and its 15-acetylated form is significantly modulated by oxidative stress in liquid cultures of *Fusarium graminearum*. FEMS Microbiol. Lett. 258, 102–107.

Poyart, C., Pellegrini, E., Gaillot, O., Boumaila, C., Baptista, M., Trieu-Cuot, P., 2001. Contribution of Mn-cofactored superoxide dismutase (SodA) to the virulence of *Streptococcus agalactiae*. Infect. Immun. 69, 5098–5106.

Proctor, R.H., Hohn, T.M., McCormick, S.P., 1995. Reduced virulence of *Gibberella zeae* caused by disruption of a trichothecene toxin biosynthetic gene. Mol. Plant Microbe Interact. 8, 593–601.

Qin, J., Wang, G., Jiang, C., Xu, J.R., Wang, C., 2015. Fgk3 glycogen synthase kinase is important for development, pathogenesis, and stress responses in *Fusarium graminearum*. Sci. Rep. 5, 8504.

Seong, K.Y., Zhao, X., Xu, J.R., Guldener, U., Kistler, H.C., 2008. Conidial germination in the filamentous fungus *Fusarium graminearum*. Fungal Genet. Biol. 45, 389–399.

Stephens, A.E., Gardiner, D.M., White, R.G., Munn, A.L., Manners, J.M., 2008. Phases of infection and gene expression of *Fusarium graminearum* during crown rot disease of wheat. Mol. Plant Microbe Interact. 21, 1571–1581.

Tang, Y., Zhang, X., Wu, W., Lu, Z., Fang, W., 2012. Inactivation of the sodA gene of *Streptococcus suis* type 2 encoding superoxide dismutase leads to reduced virulence to mice. Vet. Microbiol. 158, 360–366.

Valentine, J.S., Doucette, P.A., Zittin Potter, S., 2005. Copper-zinc superoxide dismutase and amyotrophic lateral sclerosis. Annu. Rev. Biochem. 74, 563–593.

Veal, E., Day, A., 2011. Hydrogen peroxide as a signaling molecule. Antioxid. Redox Signal. 15, 147–151.

Veluchamy, S., Williams, B., Kim, K., Dickman, M.B., 2012. The CuZn superoxide dismutase from *Sclerotinia sclerotiorum* is involved with oxidative stress tolerance, virulence, and oxalate production. Physiol. Mol. Plant Pathol. 78, 14–23.

Wang, C., Zhang, S., Hou, R., Zhao, Z., Zheng, Q., Xu, Q., et al., 2011. Functional analysis of the kinome of the wheat scab fungus *Fusarium graminearum*. PLoS Pathog. 7, e1002460.

Wu, A.B., Li, H.P., Zhao, C.S., Liao, Y.C., 2005. Comparative pathogenicity of *Fusarium graminearum* isolates from China revealed by wheat coleoptile and floret inoculations. Mycopathologia 160, 75–83.

Wu, J., Liu, Y., Lv, W., Yue, X., Que, Y., Yang, N., et al., 2015. FgRIC8 is involved in regulating vegetative growth, conidiation, deoxynivalenol production and virulence in *Fusarium graminearum*. Fungal Genet. Biol. 83, 92–102.

Yamamoto, A., Ueda, J., Yamamoto, N., Hashikawa, N., Sakurai, H., 2007. Role of heat shock transcription factor in *Saccharomyces cerevisiae* oxidative stress response. Eukaryot. Cell 6, 1373–1379.

Youn, H.D., Kim, E.J., Roe, J.H., Hah, Y.C., Kang, S.O., 1996. A novel nickel-containing superoxide dismutase from *Streptomyces* spp. Biochem. J. 318 (Pt 3), 889–896.

Yuan, T.L., Zhang, Y., Yu, X.J., Cao, X.Y., Zhang, D., 2008. Optimization of transformation system of *Fusarium graminearum*. Plant Physiol. Commun. 44, 251–256.

Zelko, I.N., Mariani, T.J., Folz, R.J., 2002. Superoxide dismutase multigene family: a comparison of the CuZn-SOD (SOD1), Mn-SOD (SOD2), and EC-SOD (SOD3) gene structures, evolution, and expression. Free Radic. Biol. Med. 33, 337–349.

Zheng, D., Zhang, S., Zhou, X., Wang, C., Xiang, P., Zheng, Q., et al., 2012. The FgHOG1 pathway regulates hyphal growth, stress responses, and plant infection in *Fusarium graminearum*. PLoS ONE 7, e49495.

Zhang, X.W., Jia, L.J., Zhang, Y., Jiang, G., Li, X., Zhang, D., et al., 2012. In planta stage-specific fungal gene profiling elucidates the molecular strategies of *Fusarium graminearum* growing inside wheat coleoptiles. Plant Cell 24, 5159–5176.